Chapter 2

Wireless Stress Sensor Based on Magnetic Microwires

Pilar Marín

Additional information is available at the end of the chapter

http://dx.doi.org/10.5772/intechopen.70354

Abstract

The development of wireless sensors and biosensors is a topic of great current interest. Amorphous magnetoelastic microwires are perfect candidates to be used as sensing elements based on two important properties, that is, magnetoelastic resonance and high-frequency giant magnetoimpedance. It was observed that such microwires present the key feature of performing magnetoelastic resonance, at the kHz range of frequency, in the absence of applied field. This fact, in addition to their small size, gives the microwires unique advantages over the widespread ribbons, currently in use as magnetoelastic sensors. The frequency, amplitude, and damping of the vibration give information of the sensor environment. On the other side, the microwire reflectivity in the microwave range can be modulated by means of magnetoimpedance effect. The maximum-induced electric current, as well as the maximum ac modulation, occurs for frequencies determined by the microwire length. The modulation also varies as a function of the dc-applied field and applied stress.

Keywords: magnetostriction, magnetoelastic resonance, high-frequency giant magnetoimpedance, amorphous magnetic microwire, biomedical sensors

1. Introduction

In recent years, much interest and effort have been devoted to develop soft magnetic materials due to their technological potential [1]. The main use of these materials can be found in the sensing industry which includes a broad spectrum of applications ranging from the automotive, mobile communication, chemistry, and biochemistry industry among many others [2–5]. Amorphous microwires are one of the most widely studied soft materials. They are fabricated by means of extracting melt-spinning Taylor technique [6]. Those microwires are composed by a metallic core and a Pyrex cover both in the micrometer range. The metallic core provides the magnetic behavior, while the cover has a protective and stress-inducting function [7]. The ratio between the total diameter and the magnetic core, often called aspect ratio, is one of the key

parameters of such microwires, since magnetic properties depend dramatically on it. For high values of the aspect ratio, the microwires present a bistable hysteresis loop, while this bistability vanishes for low ones [8, 9]. In fact, amorphous or nanocrystalline magnetic microwires are among the softest materials. Many properties of these materials have been deeply studied both from the point of view of the basic physics and the applications [10, 11]. This is the case of the giant magnetoimpedance effect [12], bistability [13], ferromagnetic resonance [14], and magnetoelastic resonance [15, 16]. It is easy, also, to find much literature regarding microwave-related applications of microwires or microwire-based materials [17–19]. Some of these articles have nicely shown how different arrangements of microwires forming arrays or embedded in different types of matrices may be used for enhancing their sensitivity as GMI elements or electromagnetic waves absorbing materials [20].

In the frequency range of GHz, some experimental and theoretical studies of the effect of the magnetization on the scattering properties of a single microwire have been recently developed [21]. This kind of work gives experimental evidence showing that the microwave scattering by a single microwire depends on the magnetic permeability with sufficient strength to be experimentally detected as an effect of the GMI. Furthermore, this dependence was also used to show the potential of such microwire as a wireless field and/or stress sensor. These experimental results are followed by a theoretical approach where the influence of the microwire magnetic state in its microwave reflection features is taken into account. Based on these studies, further experimental work shows an application of such microwire as a wireless stress sensor with the particular application of pressure detection in a hydraulic circuit simulating cardiovascular conditions [22].

Besides these investigations on magnetic microwires, it should be stated that technological development has spurred the growing interest in the investigation of new biosensors aimed at simplifying present-day diagnostic methods and thereby improving medical care, so that it improves the quality of life of the patients and allows for outpatient treatment for a number of pathologies, avoiding unnecessary hospital admissions [23]. Magnetic sensors are at the helm of technological development seen in this field over the last decades, offering numerous advantages attributed to their elevated sensitivity, reduced size, systems without the need for an external source of energy, and wireless connections. The use of wireless sensor network (WSN) technologies offers the possibility of developing implantable biomedical sensors allowing for the monitorization and follow-up of certain physiological parameters with precise and, up until now, unthinkable measurements. Based on magnetoelastic character or microwires, it has been possible to develop a wireless magnetic sensor for postoperative follow-up procedures of vascular surgery [24].

The aim of the present paper is to show the physical fundamentals and the particular applications of magnetic microwires as stress sensors

2. Scattering of electromagnetic waves by a single microwire

2.1. Magnetostrictive magnetic microwires

A magnetic microwire is a filament with an amorphous structure, whose nucleus is composed of an alloy of metals, the most frequent being iron and cobalt, with a Pyrex covering as

insulant, manufactured by means of an ultrafast cooling process resulting in microwires with a maximum total diameter around 100 m. Coils containing around 2 or 3 km of wire with a weight around 1–2 g are tailored by Taylor-Ulitovsky technique [25]. **Figure 1a** shows a photograph corresponding to a microwire scanning electron microscope (SEM) image. The composition is $Fe_{2.25}Co_{72.75}Si_{10}B_{15}$, and corresponding dimensions are a total diameter of 100 m and a metal nuclei diameter around 80 m.

Figure 2 shows a schematic diagram of the method used by Taylor-Ulitovsky. It consists of the rapid drawing of a softened glass capillary in which the molten metal is entrapped. The capillary is drawn from the end of a glass tube containing the molten alloy. Previously, a metallic pellet of the master alloy, prepared by induction melting of pure elements, has been placed inside the sealed end glass tube; then, the alloy is melted by a high-frequency field of an inductive coil, and the end of the glass tube is softened. Hence, around the molten metal drop, there is a softened glass cover which allows the drawing of the capillary. A low level of vacuum within the glass tube prevents metal oxidation. It also assures stable melt-drawing conditions, in conjunction with induction heating, employing the levitation principle. In order to ensure continuity of the process, there is a glass tube displacement with a uniform feed-in speed. The rapid cooling rate required to obtain an amorphous structure is between 10^5 and 10^6 Ks^{-1}.

Amorphous magnetoelastic Co-based magnetic microwires with negative but low magnetostriction have been used for conducting this study related with wireless stress sensing technologies. To ensure soft magnetic properties, cobalt-rich compositions, that is, $Fe_{2.25}Co_{72.75}Si_{10}B_{15}$, should be adjusted to obtain a nearly zero but negative magnetostriction constant. The

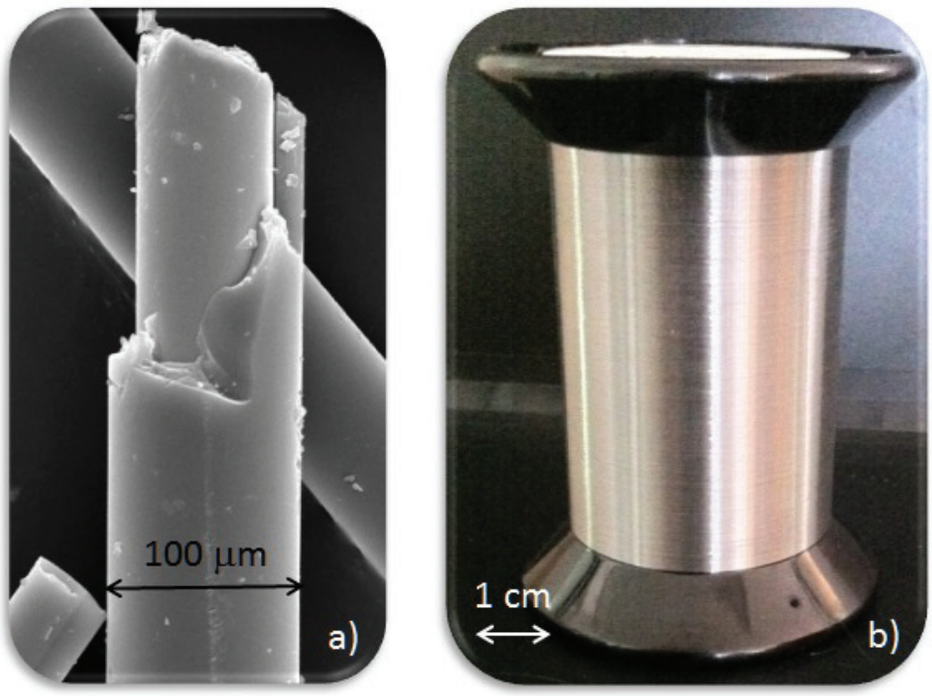

Figure 1. SEM image of an amorphous is $Fe_{2.25}Co_{72.75}Si_{10}B_{15}$ microwire (a) and photograph of coil of casted wire containing 2 g of material (b).

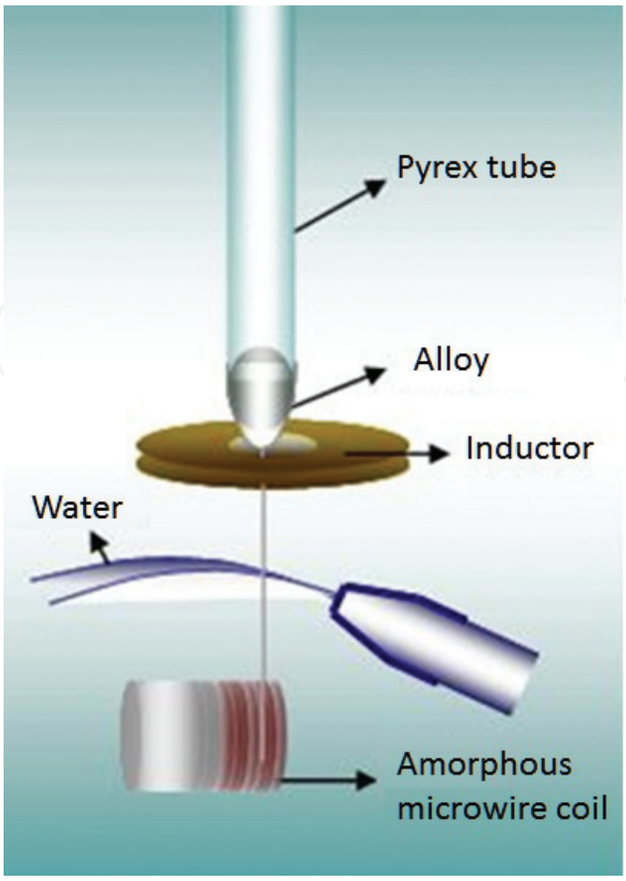

Figure 2. Microwire casting method.

bamboo-like magnetic domains observed in this type of wires have a circumferential magnetization that yields in a typical soft magnetic material hysteresis loop that exhibits low coercivity and large permeability levels [26].

Two unique characteristics which convert negative low magnetostrictive magnetic microwires into excellent sensor elements should be highlighted. On the one hand, their high magnetostriction, together with their low anisotropy, makes them extremely sensitive to small changes in mechanical stress and that such changes be translated into changes in their magnetization when subjected to an external magnetic field. In addition, because of its high magnetic susceptibility along with its diameter in microns, it is able to modulate a high-frequency signal emitted by an antenna. Thus, changes in stress or pressure of a fluid will cause a variation of the mechanical stress on the sensor, which will involve a variation of its magnetization and the emitted wave that will be detectable wirelessly through a receiving antenna [27].

Microwires' magnetic hysteresis loops are easily detected using experimental setups consisting of a primary and a secondary coil by a conventional low-frequency induction technique. The stress influence on microwire magnetic behavior can be quantified by means of hysteresis loop evolution when tensile stresses are applied to the microwire by means of hanging different weights. **Figure 3** shows the evolution of $Fe_{2.25}Co_{72.75}Si_{10}B_{15}$ hysteresis loops with tensile

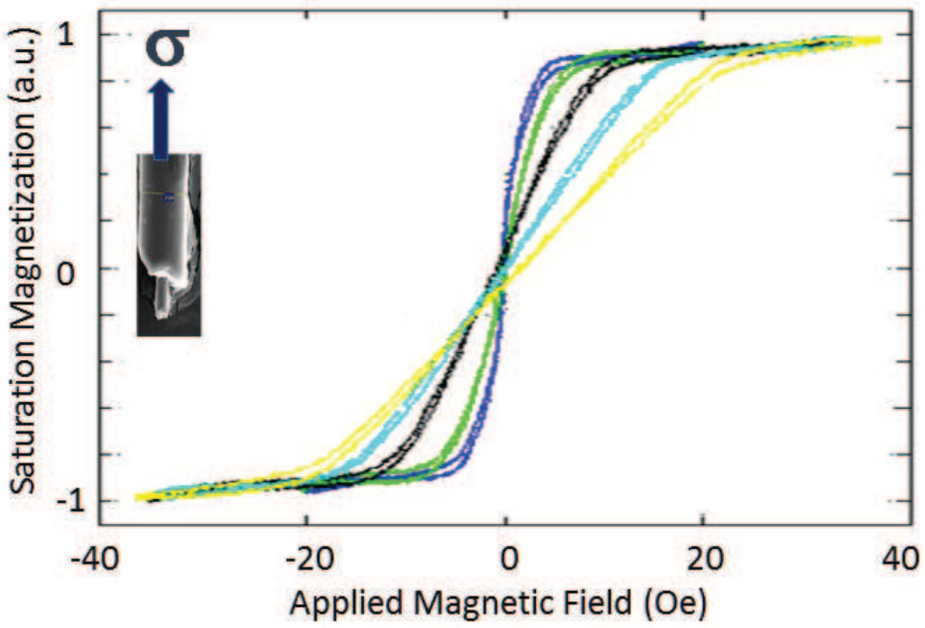

Figure 3. Stress influence on microwire hysteresis loop: 0 (■), 112 (■), 345 (■), 580 (■), and 813 (■) MPa.

stress, from 0 to 813 MPa. Magnetostrictive character of magnetic microwires is observed by means of a clear decrease of magnetic susceptibility with increasing tensile stress.

2.2. Tuned scattering of electromagnetic waves by a finite length ferromagnetic microwire

The metallic nature of ferromagnetic microwires determines the characteristics of their interaction with electromagnetic waves. An alternating electric field E_{inc}, with frequency ω, that is, at the Gigahertz range, and parallel to the axis of the wire and uniform along its length, excites the microwire inducing an electric current I(z) along the microwire. The total electric field E, at any point of the space, can be obtained as the sum of both contributions, that is, $E = E_{inc} + E_{sca}$, where E_{sca} is the electric field generated by the induced current in the thin wire. Following the antenna theory, the electric current can be computed by the Hallen equation [28]:

$$2i\int_{-\frac{L}{2}}^{\frac{L}{2}}\left(Z_0\frac{e^{-ik|r-r'|}}{4\pi|r-r'|}+Z_i e^{-ik|z-z'|}\right)Idz' = C_1 sinkz + C_2 coskz + 2\frac{E_0}{k} \quad (1)$$

where Z_0 the medium impedance, C_1 and C_2 are arbitrary constants fixed by the boundary conditions I(L/2) = I(−L/2) = 0, k is the wave vector, and E_0 is the amplitude of the microwave electric field. The wire impedance per unit length, Z_i is given by Eq.(2). It depends on the magnetic permeability of the microwire according to its general expression [29]:

$$Z_i = \sqrt{\frac{\omega\mu}{2\sigma}}\frac{(1-i)J_o\left(\frac{(1-i)a}{\delta}\right)}{2\pi a J_1\left(\frac{(1-i)a}{\delta}\right)} \quad (2)$$

where J_o and J_1 are the first-kind Bessel functions, $\delta = \sqrt{2/\omega\mu\sigma}$ is the magnetic skin depth [30], $2a$ is a characteristic cross-sectional size, and σ and μ hold for the electrical conductivity and the magnetic permeability of the microwire, respectively. It is important to remark that although the magnetic permeability of a microwire is strictly a tensor magnitude [30–32], for simplification and as an approximation, the magnetic permeability was taken as a scalar magnitude [33]. A more general treatment about the relation among the magnetic permeability and the electric impedance of a microwire can be seen in Refs. [34, 35]. Nevertheless, the most important issue related to the induced current in a magnetic microwire holds in the Z_i expression, given by Eq. (2) and its own dependence on the magnetic permeability that can be dramatically changed in ferromagnetic microwires by applying a bias magnetic field [36].

In order to quantify the total induced current, I(z), in magnetic microwires in the presence of microwaves verifying the integral equation, Hernando et al. [37] have applied a pulse function point matching method [35] for microwires with radius a = 33 μm, electric conductivity of order of 10^7 S, relative magnetic permeability value of 2, and an amplitude of the electric field about 1 V/m. As previously mentioned, the boundary conditions were applied on the electric current to set the values of the constants C_1 and C_2. Furthermore, the effect produced in the induced current by variations of the microwire magnetic permeability at different microwave frequencies was also studied. **Figure 4** shows the modulus $I(z)$ at the center of different microwires, $I(0)$, with lengths of 5, 10, 15, and 30 cm as a function of the microwave frequency for different values of the magnetic permeability.

The results clearly show a current distribution typical for thin metallic wires, where the electric current is maxima at certain frequencies depending on the length of the wire: dipole antenna resonances. The maximum $I(0)$ variation induced by changes of the magnetic permeability is shown to correspond to that obtained at the dipole antenna resonances. Consequently, maximum giant magnetoimpedance effect will be achieved at these resonance frequencies.

In order to corroborate the proposed theoretical model, microwave characterization of 33 μm radius Co-based microwires and different lengths was carried out in the 500 MHz–2 GHz frequency range. The microwave scattering properties of these magnetic microwires were experimentally analyzed, as shown in **Figure 5**, by using two helical antennas (with 21.5 cm of length, 3 cm of radius, central frequency of 1 GHz, and a wave band of 500 MHz) connected to a Programmable Network Analyzer from Agilent Ltd., working in the frequency range comprised between 10 MHz and 20 GHz. Furthermore, a microwave polarizer was used to ensure that the electric field of the microwave was parallel to the axis of the microwire. The experiments were based on S_{ij} parameter measurements defined as shown in Eq. (3) where P_1 and P_2 stand for the input and output signal, respectively:

$$S_{ij} = 20log_{10}\frac{P_i}{P_j}; i, j = 1, 2 \tag{3}$$

In our case, we restricted the study to the S_{21} parameter. The choice was based in the interesting physical meaning, since it represents the measured power in the receiving antenna over the outgoing power in the emitting one.

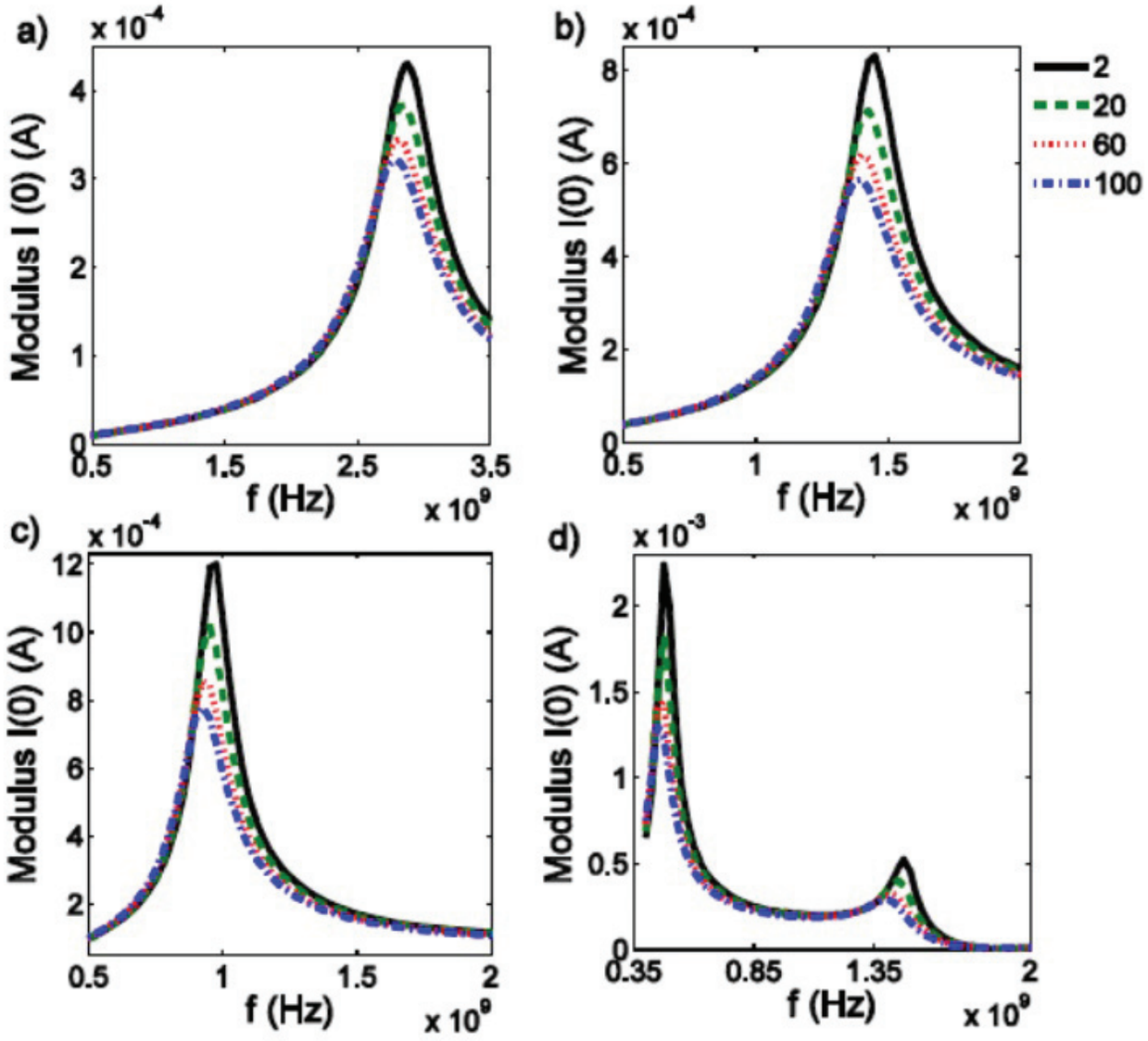

Figure 4. Frequency spectrum of the modulus of the electrical current at the center of a microwire for different relative, permeabilities for (a) 5 cm, (b) 10 cm, (c) 15 cm and (d) 30 cm microwire length where 2, 20, 60, and 100 are values of permeability. (Figure published with copyright permission from IEEE Transactions on Antennas and Propagations. 2016;64(3):1112-1115).

It is important to take into account that the scattering coefficient is directly related to the electrical current induced along the microwire by the incident wave since the scattered wave is generated by the electric current along the microwire (1) (the field distribution corresponds for a dipole antenna [35]).

As previously demonstrated (**Figure 4**), the electric current can be modified changing the magnetic permeability of the ferromagnetic microwire. For this reason, two Helmholtz coils were used to apply an ac-bias magnetic field, parallel to the axis of the microwire, with amplitude of 2.7 Oe and a frequency of 10 Hz. The experiments were performed by applying a dc magnetic field in addition to the abovementioned ac-bias magnetic field, also parallel to the axis of the microwire. Following this procedure, the modulation is driven around different points of the hysteresis loop or different magnetic states. The ac field also gives rise to a

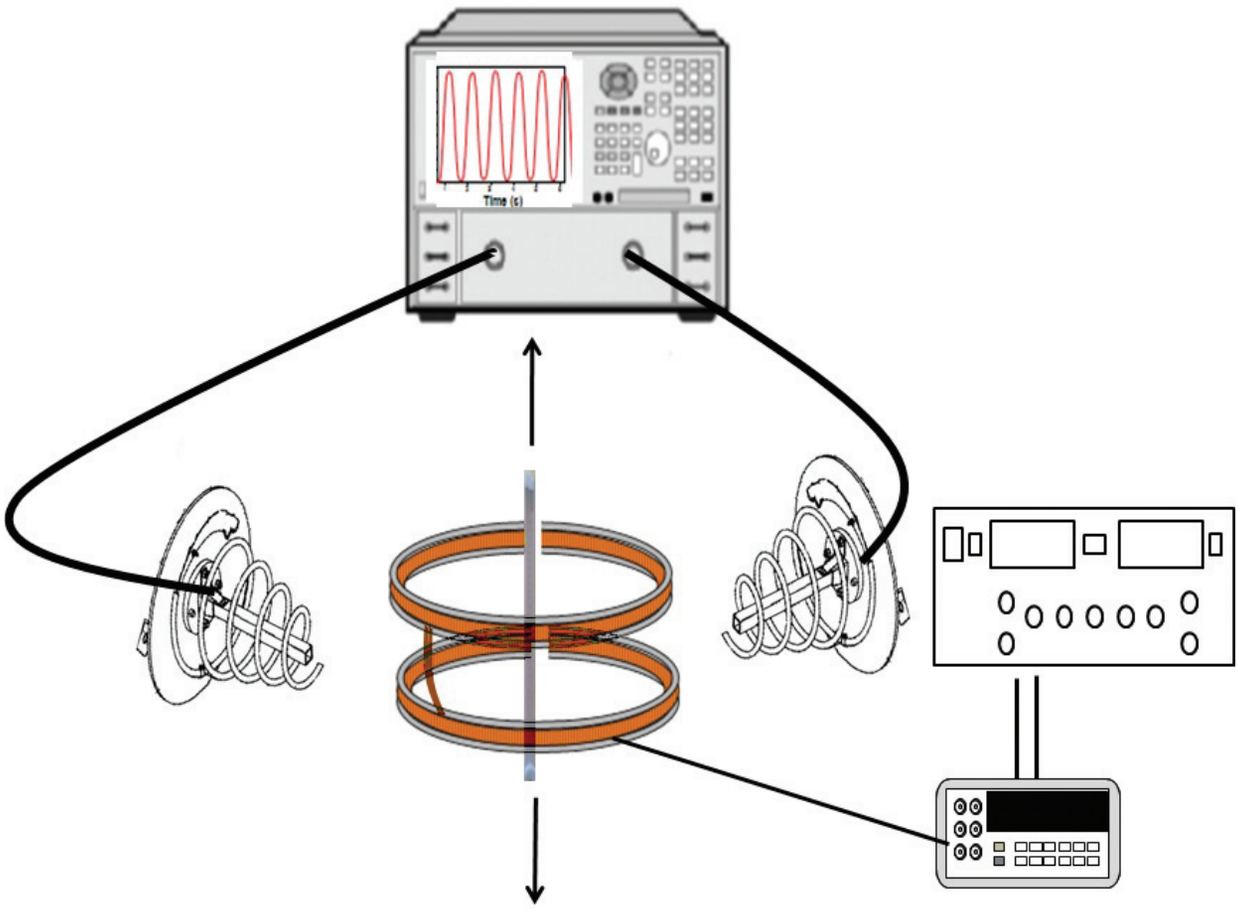

Figure 5. Experimental setup for combined application of high-frequency electromagnetic wave with frequency between 10 MHz and 20 GHz by means of helicoidally antennas connected to Programmable Network Analyzer and 10 Hz low-frequency bias field using Helmholtz coils.

modulation of the microwire permeability that is reflected as a modulation in the scattering coefficient: ΔS21. The amplitude of the modulation of the scattering coefficient due to the ac-bias field as a function of the dc-applied field for a 10 and 15 cm microwire length is represented in **Figure 6**.

In the insets of **Figure 6**, the microwave spectrum for each microwire length at zero dc field is depicted. For each case, a maximum variation of the amplitude of the modulation induced in the scattering coefficient at the following frequencies, 1.4 GHz for the 10 cm length (**Figure 6a**) and 1 GHz for the 15 cm microwire length (**Figure 6b**), is observed. This experimental feature perfectly matches with the antenna resonance frequencies deduced by numerical calculations as shown in **Figure 4**.

At constant frequency the scattering coefficient modulation increases as the dc-applied field, reaching a maximum, at 3 Oe for both microwires length. This field corresponds to the experimental coercive field measured at 10 Hz by typical induction measurements (see **Figure 7**) [27].

Effectively, the maximum permeability variation induced by an applied field is expected to occur when the latter equals the coercivity of the wire. For dc magnetic fields larger than *3 Oe*,

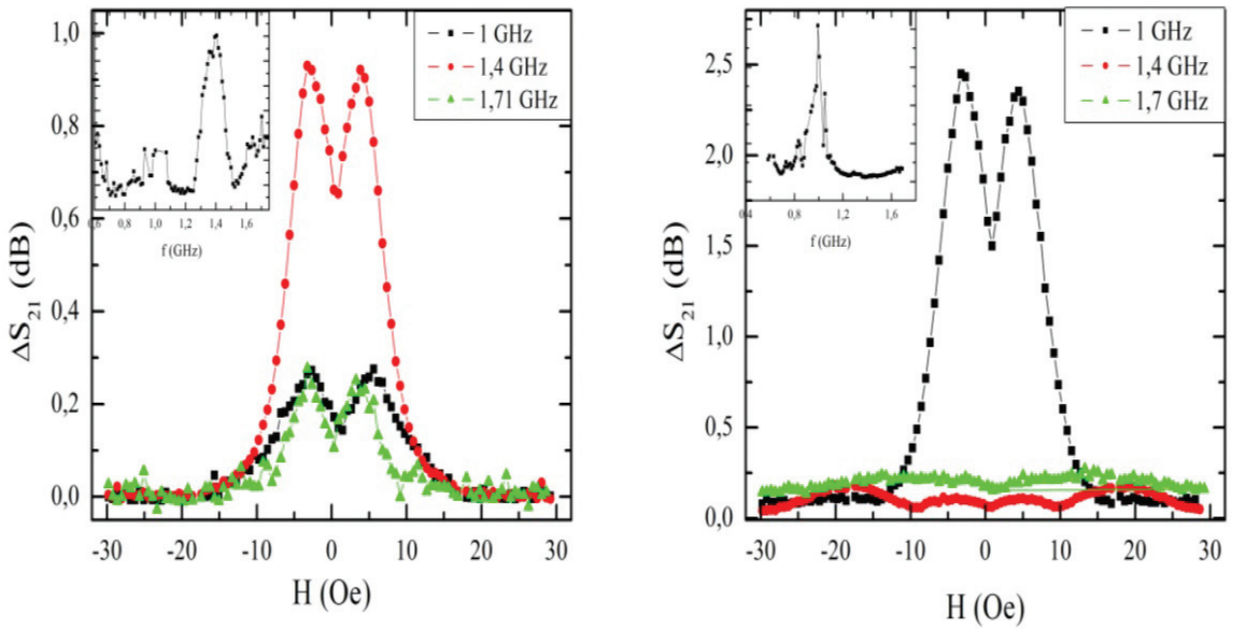

Figure 6. Relative variation of the scattering coefficient S_{21} as a function of the applied dc-bias field for (a) a 10-cm microwire length where the maximum variation occurs at 1.5 GHz and (b) a 15-cm-microwire length where the maximum variation occurs at 1 GHz. In the insets the microwave spectrum for each microwire at zero dc-bias field is represented [37] (Figure published with copyright permission from IEEE Transactions on Antennas and Propagations. 2016;64(3):1112-1115).

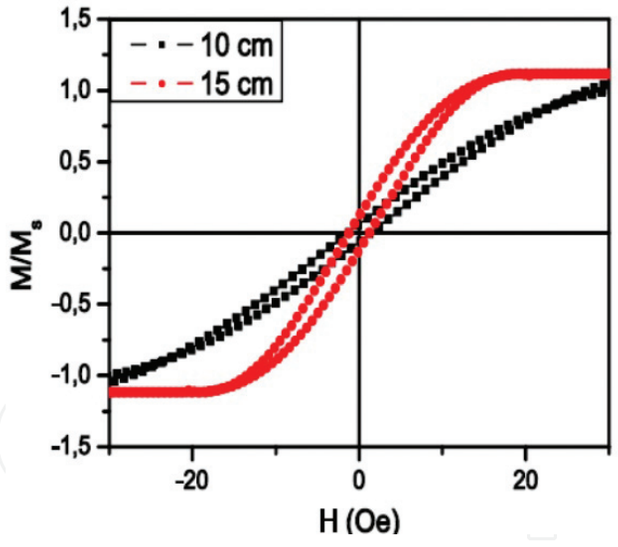

Figure 7. Hysteresis loops for Co-rich microwires with negative magnetostriction at 10 Hz measured by ac induction technique with 10 and 15 cm length, respectively (adapted from Hernando et al. [37]).

the modulation of the scattering field diminishes and finally vanishes for dc fields well above the saturation field (the impedance, Z_i, of the magnetic microwire is not modulated because of the magnetic permeability that remains constant). Therefore, it has been shown in the experiments that the maximum changes in the microwave spectrum by the GMI occur at the antenna resonances as was shown applying the antenna theory. The curves shown in **Figure 6**

suggest that at the dipole resonance the system can be used as a sensitive detector of magnetic fields. This effect can be used for different sensing applications.

2.3. Stress and field contactless sensor based on the scattering of electromagnetic waves by a single ferromagnetic microwire

The following paragraphs [38] present experimental evidence that the microwave scattering by a single microwire depends on the magnetic permeability with sufficient strength to be experimentally detected as an effect of the GMI. Furthermore, this dependence has been also used to show the potential of such microwire as a wireless field and/or **stress sensor**.

A 10-cm-length sample of magnetostrictive $Fe_{2.25}Co_{72.75}Si_{10}B_{15}$ amorphous microwire, presenting high magnetoimpedance effect, of metallic core radius of a = 33 μm and total radius, including the Pyrex outer shell, of 50 μm was placed between two helical antennas working in the GHz range with circular polarized radiation as shown in **Figure 5**. As previously stated in the present work, due to its amorphous structure, even though they exhibit low or moderate magnetostriction, highly sensitive magnetoelastic elements for detecting applied stresses are thoroughly discussed elsewhere since long time ago [39].

Figure 8 displays the experimental result of measuring the S_{21} parameter over time for the aforementioned setup with an emission frequency of the antennas set at $f_{antennas}$ = 1.2 GHz. The modulation of the S_{21} parameter shown in **Figure 8** is produced by the application of a bias field with frequency f_{bias} = 100 mHz. Note that the modulated signal shows a frequency of f_{mod} = 200 mHz, which is exactly twice the value of the bias frequency. This result suggests that the scattering is being somehow tuned by the magnetization of the sample, more precisely by

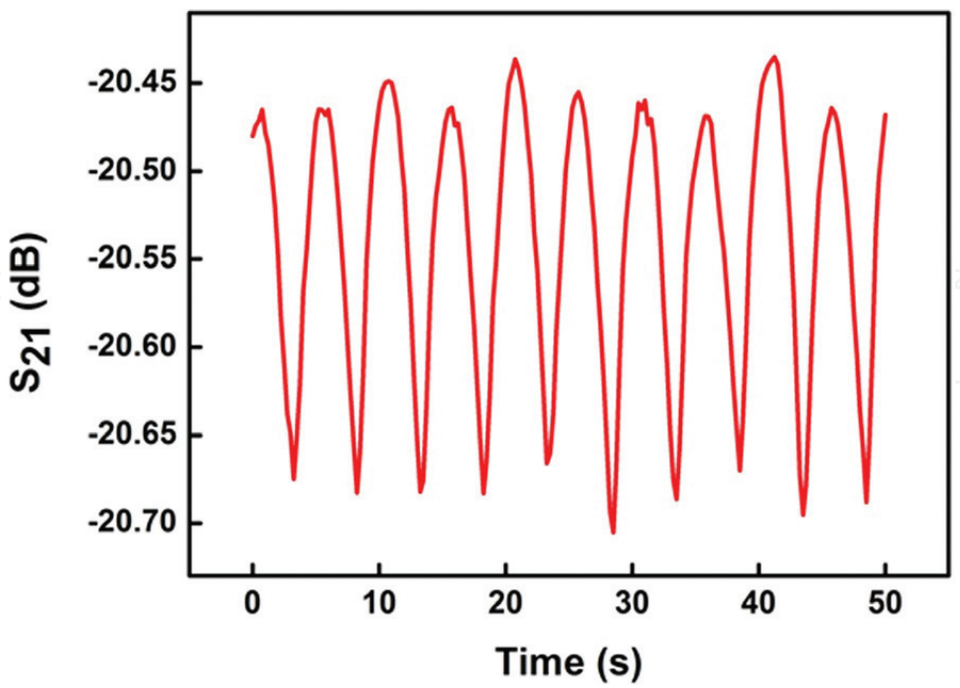

Figure 8. Experimental S_{21} parameter time evolution for the experiment depicted in **Figure 5** with $f_{antennas}$ = 1.2 GHz and f_{bias} = 100 mHz.

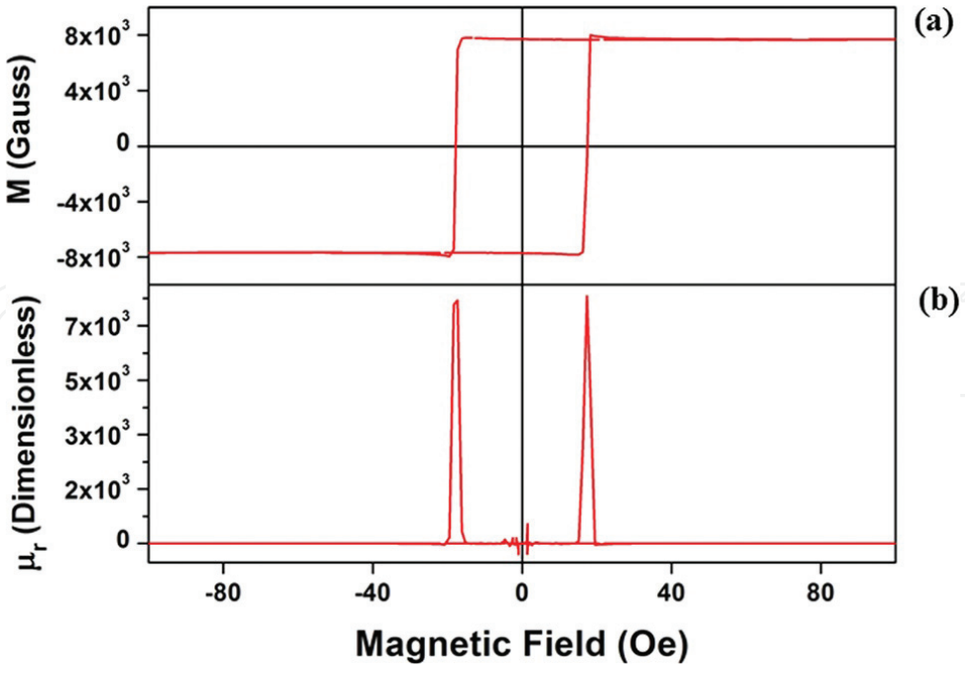

Figure 9. (a) Hysteresis loop of the $Fe_{2.25}Co_{72.75}Si_{10}B_{15}$ sample. (b) Relative magnetic permeability of the $Fe_{2.25}Co_{72.75}Si_{10}B_{15}$ sample.

its magnetic permeability μ_r. This doubled frequency is due to the symmetric shape of the microwire hysteresis loop ($|\mu_r(H_{bias})|$) = $|\mu_r(-H_{bias})|$, as can be seen in **Figure 9** in which the experimental hysteresis loop of the wire, measured using a quantum design vibrating sample magnetometer, as well as the low-frequency permeability, which reaches values of 8×10^3, has been plotted.

Moreover, the use of even a weak magnetostrictive microwire, as the one chosen, allows us to modify its magnetic permeability by application of mechanical stresses. **Figure 10** displays the result of an analogous experiment as the one depicted in **Figure 5** but with the addition of a tensile device. Such device allows the application of different mechanical stresses to the microwire during the experiment. It can be noticed how the modulated pattern of S21 is

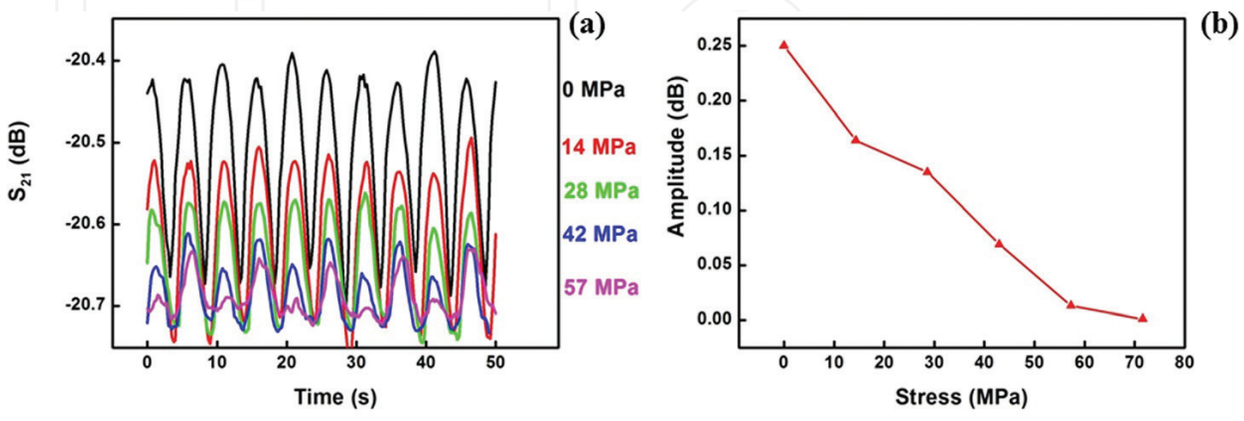

Figure 10. (a) Experimental S_{21} parameter time evolution for the $F_{2.25}Co_{72.75}Si_{10}B_{15}$ microwire subjected to different mechanical stresses. (b) Peak-to-peak amplitude of the S_{21} modulated signal as a function of the applied mass load (Figure published with copyright permission from Appl. Phys. Lett. 2014;105:092505(1)-092505(4)).

modified under the application of the different mechanical stresses. In this case, the application of the stress induces a magnetoelastic anisotropy, with strength given by the product of the stress and the magnetization constant, which decreases the relative permeability, μ_r, of the microwire.

The physical aspects underlying the experiments reported here are as follows. The modulation of S_{21} parameter observed in **Figures 2** and **4** describes the modulation of the reflected power P_2 at the receiving antenna position. The intensity of the wave reflected or scattered by the microwire shall depend on its impedance Z_2 as shown in Eq. (2). According to Eqs. (2) and (3), the bias field induces periodic changes of S_{21} as a consequence of the modulation that this field produces on μ_r as described by **Figure 8**. The periodic variation of μ_r gives rise through Eq. (2) to Z_2 and P_2 modulations that finally originates the experimental behavior summarized in **Figures 8** and **10**. The figure of merit, β, which we are interested in, is given by the following expression:

$$\beta = \frac{\Delta S_{21}}{S_{21}} = \alpha \Delta \mu_r \tag{4}$$

where ΔS_{21} is the change of S_{21} originated by a change in permeability of strength $\Delta\mu_r$. Accordingly to previous considerations, the parameter should be estimated through the dependence of both S_{21} on P_2 and from that of Z_2 on P_2.

The last one may be derived after using a standard method for calculating the scattering of electromagnetic waves by cylindrical ideal conductors that can be found elsewhere in the bibliography [40]. Such procedure is strictly based on solving the boundary conditions of the incident and reflected fields at the interphase r = a that in our case is the radius of the microwire metallic core. If we use the same geometry than in standard calculations [40] but considering a cylinder with finite conductivity and after expressing the magnetic and electric fields as linear combinations of Bessel, I_i, and Hankel, H_i, functions, their boundary conditions yield, for the transversal magnetic (TM) and transversal electric (TE) cases, reflection coefficients ($\widetilde{a_i}^{TE}$, $\widetilde{a_i}^{TM}$) of the Hankel, $H_i(k_1 r)$, functions describing the outgoing scattered wave [38]. Contrary to the perfect conductor, reflection coefficients, $\widetilde{a_i}^{TE}$ and $\widetilde{a_i}^{TM}$, both function on Z_2 and k_2 which, in turn, are dependent on the magnetic permeability (see Eq. (2) and the following expression):

$$k_2 = \sqrt{i\omega\sigma\mu_0\mu_r} \tag{5}$$

Thus, it is possible to change $\widetilde{a_i}^{TE}$ and $\widetilde{a_i}^{TM}$ by tuning the magnetic state of the cylinder.

Some estimative considerations are outlined for a first-order approximation that corresponds to the case in which only a_0 coefficients are relevant. In order to establish the correlation between the experimental parameter S_{21} and the theoretical scattering coefficients $\widetilde{a_0}^{TE}$ and $\widetilde{a_0}^{TM}$, we formulate the S_{21} parameter as a function of the scattering coefficients $\widetilde{a_0}^{TE}$ and $\widetilde{a_0}^{TM}$, by expressing the input and output power in Eq. (4) as the average value of the Poynting vector in the positions corresponding to both antennas. The explicit dependence of S_{21} with the theoretical scattering parameters is given by the following expression:

$$S_{21} = 20log_{10}\left(\frac{\left(1+\widetilde{a_0}^{circ}(\mu_r)\right)E_{in}^{i}(kr_2)}{E_{in}^{i}(kr_1)}\right)^2 \tag{6}$$

where E_{in}^{i} stands for the incident electric field; r_1 and r_2 represent the positions of the emitting and receiving antennas, respectively; and $\widetilde{a_0}^{\text{circ}}$ stands for the scattering parameter for circular polarized radiation. e $\widetilde{a_0}^{\text{circ}}$ can be estimated as the mean value of the TE and TM modes.

In summary, it has been experimentally shown that the microwave scattered intensity produced by a single microwire can be controlled by tuning its permeability. This permeability may be modified with the application of an external bias field, leading to non-negligible effects in the scattering. In addition, if the cylinder is magnetostrictive, the scattering is also sensitive to mechanical stresses. These experimental results are promising for developments in this field including in situ and in vivo biomedical magnetoelastic experiments, taking advantage of the biocompatible nature of the microwire Pyrex cover. So far, these kinds of measurements were only possible by using GMI or magnetoelastic resonance-based devices. However, the use of GHz frequency devices would allow the development of sensors operating at much longer distances and with a higher information transfer rate.

2.4. Liquid pressure wireless sensor based on magnetostrictive microwires for applications in cardiovascular localized diagnostics

The present work shows an application of such microwire as a wireless stress sensor with the particular application of pressure detection in a hydraulic circuit simulating cardiovascular conditions.

Two kinds of experiments have been performed. Both using a $Fe_{2.25}Co_{72.75}Si_{10}B_{15}$ amorphous magnetostrictive microwire with negative magnetostriction constant $\lambda_s = -0.9 \times 10^{-6}$ and saturation magnetization, $\mu_o M_s$ = 1.1 T of metallic core radius of a = 33 μm, and total radius, including the Pyrex outer shell, of 50 μm. The coercive field measured under a 10 Hz applied field is 3 Oe. The relative permeability of the microwire changes between 800 and 2 when the applied field varies between 0 and 20 Oe, 30, respectively. We selected this composition because, as stated above, Co-rich microwires are well known to exhibit a noticeable high GMI effect [32].

The first experiment consists in tagging a silicon test tube (**Figure 11(a)**) with a single microwire, in order to show the possibility of using this kind of material as a contactless strain-sensing element. The second one has been designed to test the possibilities of this material to detect changes of the blood flow pumping both in an endovascular prosthesis and in an artery. With this second aim, either a piece of an artery or prosthesis (**Figure 11(b)**) sensorized by means of a ring of Co-based magnetostrictive microwire is placed in a hydraulic circuit connected to a pulsatile ventricular assist system (Abiomed/AB5000). A water seal and two resistors in parallel have been situated in order to control over fluid pressure. The hydraulic circuit described allows a fluid flow pumping frequency of 40/60 = 0.666 Hz, which is a signal with a period of 1.5 s corresponding to a pump of 40 beats/min. A solution of 0.33% agar has been used to make the fluid through the circuit to have a similar blood viscosity at 37°C. In order to register, instantaneously, the fluid pressure through the circuit of two probes, connected to a pressure detector, was invasively connected in distal and proximal positions, respectively, with respect to the sensing element (microwire ring). Fluid pressure can be calculated as a ratio between these two values.

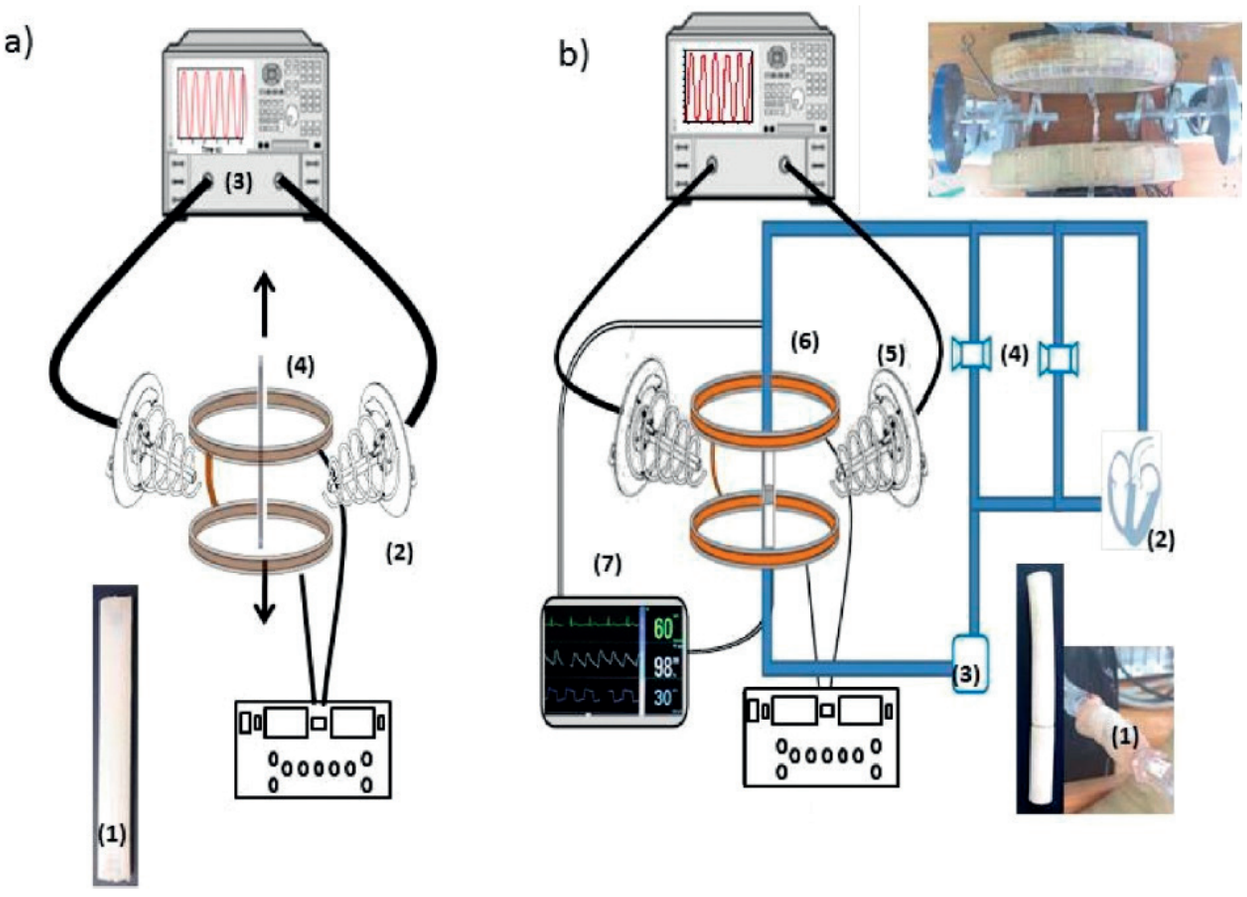

Figure 11. Experimental setups (a) on silicon test tube (1) under stress where emitting and receiving antennas (2) are connected to spectrum analyzer (3) and Helmholtz coils generate low-frequency magnetic field (4); (b) to detect changes of the blood flow pumping both in an endovascular prosthesis and in an artery. A piece of an artery or prosthesis (1) sensorized by means of a ring of Co-based magnetostrictive microwire placed in a hydraulic circuit connected to a pulsatile ventricular assist system (Abiomed/AB5000) (2), water seal (3), and two resistors in parallel (4) to control over fluid pressure, emitting and receiving antennas (5), Helmholtz coils (6), and invasive pressure detector (7) (Figure published with copyright permission from AIP ADVANCES5, 087132 (2015)).

Both specimens, sensorized silicon test tube (see **Figure 11a**) and endovascular prosthesis or artery connected to the hydraulic circuit (see **Figure 11b**), were placed between two helical antennas working at 1.2 GHz with circular polarized radiation. Both antennas were connected to a two-port Agilent E8362B Network Analyzer. The distance between antennas was large enough to ensure that a human body could be comfortably placed between them and that the far-field contribution dominates the near-field one. In addition to that, two Helmholtz coils with a customized electronic setup were used to apply an ac-bias magnetic field. Such experimental arrangement allows us to measure the scattering parameters of the system S_{21}.

Figure 12a displays the experimental result of measuring the S_{21} parameter over time for the aforementioned setup in the case of the first experiment with an emission frequency of the antennas set at $f_{antennas}$ = 1.2 GHz. The modulation of the S_{21} parameter shown in **Figure 12a** is produced by the application of a bias field with frequency f_{bias} = 100 mHz although the modulated signal shows a frequency of f_{mod} = 200 mHz, which is exactly twice the value of the bias frequency due to the tuning of the scattering by sample magnetization. Moreover, the

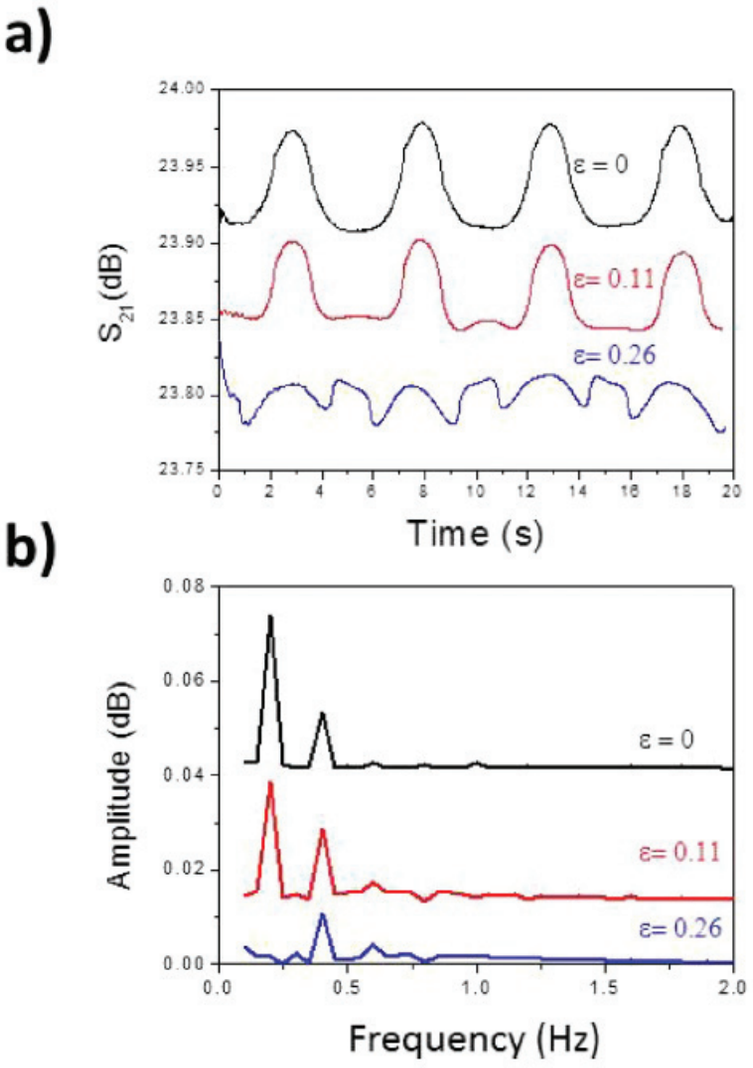

Figure 12. Influence of strain on silicon test tube on scattering attenuation coefficients, S_{21}, as a function of time (a) and corresponding fast Fourier transformation (FFT) curves (b).

use of even a weak magnetostrictive microwire, as the one chosen, allows us to modify its magnetic permeability by application of mechanical stresses. It can be noticed how the modulated pattern of S_{21} is modified under the application of the different mechanical stresses and correlated with the silicon test tube strain.

As shown in Ref. [38], the application of the stress induces a magnetoelastic anisotropy, with strength given by the product of the stress and the magnetization constant, which decreases the relative permeability, μ_r, of the microwire. **Figure 12b** shows the fast Fourier transform of curves in **Figure 12a** to quantify the frequency and amplitude of the signals. Two frequencies are observed, 200 and 400 mHz, respectively, with a clear amplitude decrease for the first one as a function of test tube strain, while the second one remains almost constant. From these data the relationship between the silicon strain and the reflectivity of the microwire can be roughly estimated. A reflectivity decrease of 0.033 dB is associated to a strain $\varepsilon = 0.26$.

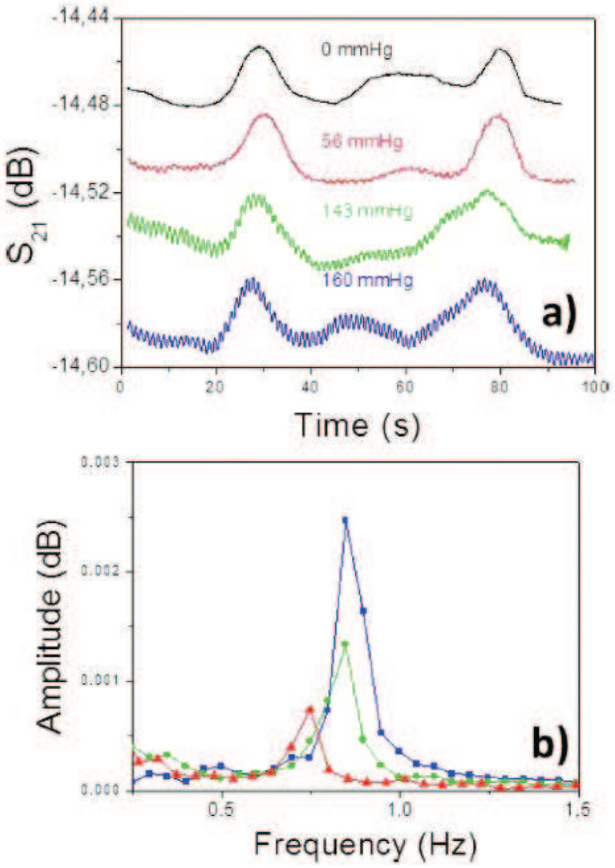

Figure 13. Experimental results of measuring the S_{21} parameter in the case of the sensorized arterial prosthesis using 1.2 GHz and a bias field frequency f_{bias} = 8 mHz as the function of fluid pressure (a) and corresponding fast Fourier transformation (FFT) (b) for 56 mmHg (▲), 143 mmHg (•), and 160 mmHg (■) (Figure published with copyright permission from AIP ADVANCES5, 087132 (2015)).

Figure 13a shows the experimental results of measuring the S_{21} parameter in the case of the sensorized arterial prosthesis using 1.2 GHz and a bias field frequency f_{bias} = 8 mHz as function of fluid pressure (from 0 to 160 mmHg). An initial modulated signal of 16 mHz is observed, but, as the pressure increases, a second superimposed signal with a frequency of 666 mHz can be seen. The amplitude of this second signal increases as fluid pressure grows (see the inset in **Figure 13**).

A crucial point in this experiment should be noted. This is the relationship between the frequencies of the bias field and the fluid flow pumping. Only a very low value of bias field frequency allows the observation of the effect. In this case the fast Fourier transformation (FFT) in **Figure 13b** shows two main peaks: the first one at 16 mHz with no sensible variation due to pressure and a second one at around 700 mHz strongly affected by pressure changes.

The same experiment has been performed in a bovine artery for fluid pressure between 100 and 235 mmHg. **Figure 14** shows pressure influence on S_{21} parameter as a function of time under the same conditions of the previous case of the prosthesis. The greater flexibility of the artery is clearly shown in the evolution of the fast Fourier transform of these signals with increasing system pressure.

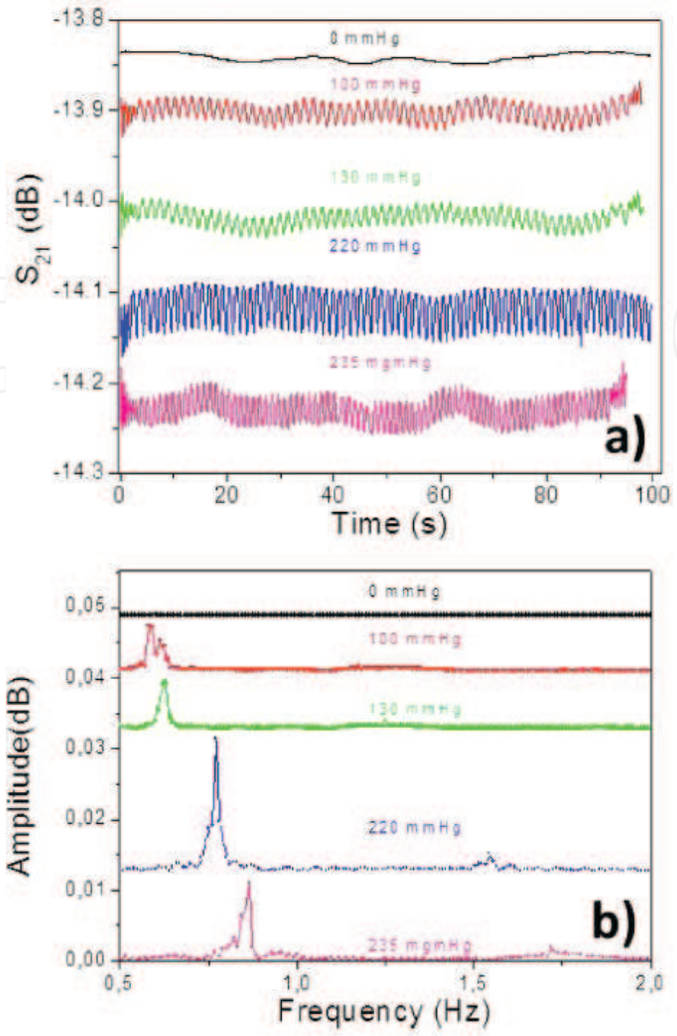

Figure 14. Experimental results of measuring the S_{21} parameter in the case of the sensorized bovine artery using 1.2 GHz and a bias field frequency f_{bias} = 8 mHz as function of fluid pressure (a) and corresponding fast Fourier transformation (FFT) (b) for 56 mmHg (▲), 143 mmHg (•), and 160 mmHg (■) (Figure published with copyright permission from AIP ADVANCES5, 087132 (2015)).

Figure 15 compares reflectivity versus pressure for both elements where the same changes in the fluid pressure involve higher increment in reflectivity for the artery in concordance with its higher elasticity.

In conclusion, we proposed the flexible magnetic element able to be integrated both in artery and prosthesis suitable for wireless localized blood pressure monitoring [22]. The sensor made of a ring of glass-covered magnetic microwire is simple and inexpensive and could be detected by means of a simple exciting and detecting set up able of emitting and detecting microwaves simultaneously applying a low-frequency magnetic field. The reflectivity of the microwire is determined by mechanical changes. In the experimental study, a piece of a cardiovascular prosthesis and a piece of an artery both sensed with a ring of magnetic microwire have been situated in a hydraulic setup simulating cardiovascular human circuit. Reflectivity changes of the sensor show its capability of measuring pressure variations in the circuit.

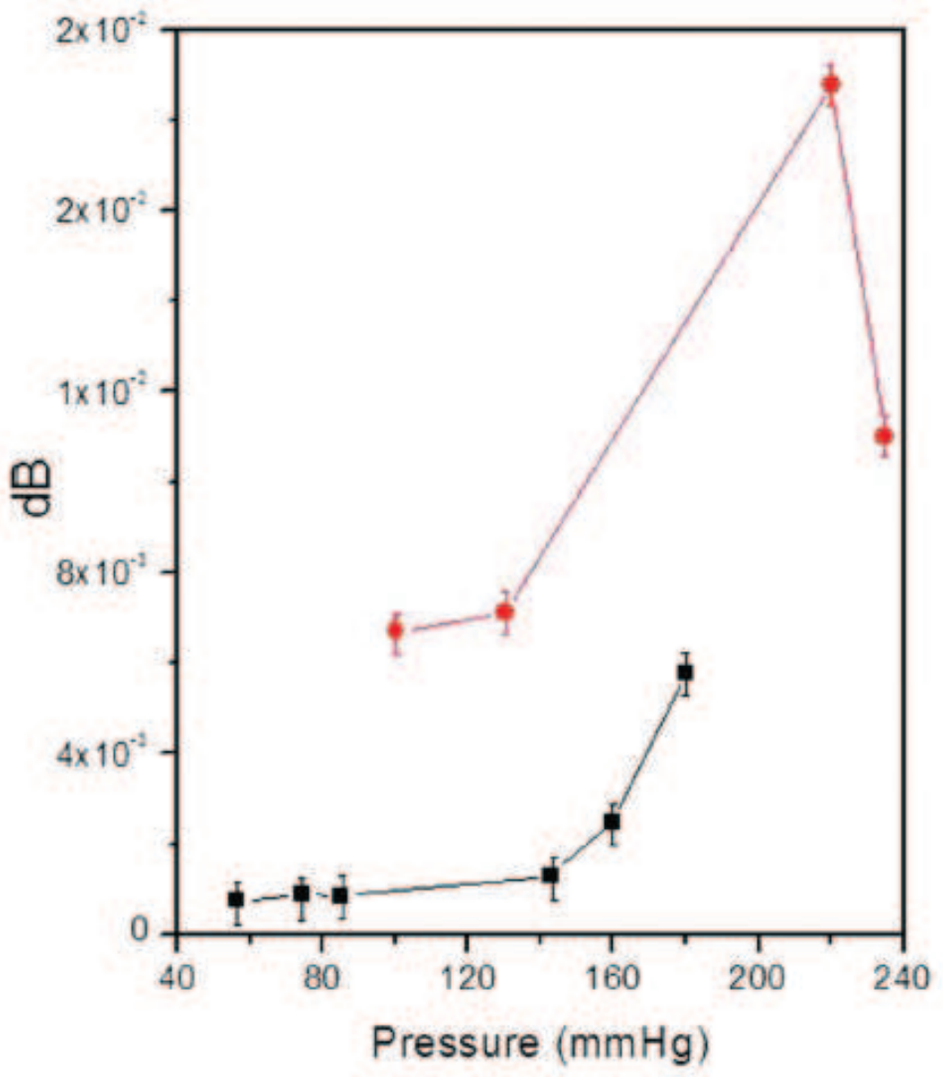

Figure 15. Reflectivity versus pressure for sensorized arterial prosthesis (■) and bovine artery (•) (Figure published with copyright permission from AIP ADVANCES5, 087132 (2015)).

3. Conclusions

In conclusion, an electromagnetic field induces an electric current along the microwire that can be modulated by the application of an external ac magnetic field, an effect known as magnetoimpedance. The maximum induced electric current, as well as the maximum ac modulation, occurs for frequencies determined by the microwire length. The modulation also varies as a function of the dc-applied field and takes a maximum when the dc field is close to the coercivity of the microwire. In fact, when the dc-field strength equals the coercive field, the variation of the permeability induced by the ac-superimposed field reaches a maximum value. This effect can be used for different sensing applications.

It is also interesting to note that for driving field frequencies corresponding to magnetoelastic or ferromagnetic resonance frequencies of microwires, small variations of the applied field or stress can give rise to strong changes in permeability. In order to increase the sensitivity of the

system, it is also important to select the frequency in that range for which the couple of antennas is close to resonance in wires.

It must be noticed that we had outlined an estimation of the wire sensitivity without considering the tensor form of the permeability at the microwave range. A more rigorous analysis could be carried out, but to account for the order of magnitude of the experimental results reported in this work, the considered approximation seems to be sufficiently illustrative.

In summary, it has been experimentally shown that the microwave scattered intensity produced by a single microwire can be controlled by tuning its permeability. This permeability may be modified with the application of an external bias field, leading to non-negligible effects in the scattering. In addition, if the cylinder is magnetostrictive, the scattering is also sensitive to mechanical stresses. These experimental results are promising for future developments in this field including in situ and in vivo biomedical magnetoelastic experiments, taking advantage of the biocompatible nature of the microwire Pyrex cover.

Acknowledgements

The author wants to acknowledge the Spanish Ministry of Economy and Competitiveness for its support via the projects MAT2013-49847-EXP and MAT2015-67557-C2-1-P and Comunidad de Madrid for support S2013/MIT-2850 NANOFRONTMAG-CM.

Author details

Pilar Marín

Address all correspondence to: mpmarin@fis.ucm.es

Departamento de Física de Materiales, Instituto de Magnetismo Aplicado, Universidad Complutense de Madrid, Spain

References

[1] Marín P, López M, Agudo P, Vázquez M, Hernando A. Applications of amorphous samples presenting high magnetomechanical coupling during the first stages of nanocrystallisation process. Sensors and Actuators A: Physical. 2001;**91**(1-2):218-222. DOI: https://doi.org/10.1016/S0924-4247(01)00464-2

[2] Vázquez M. Handbook of Magnetism and Advanced Magnetic Materials. In: Kronmuller H, Parkin S, editors. United Kingdom: Wiley, Chichester; 2007. pp. 2193-2226

[3] Chiriac H, Tibu M, Moga AC, Herea DD. Magnetic GMI sensor for detection of biomolecules. Journal of Magnetism and Magnetic Materials. 2005;**293**(1):671-676. DOI: https://doi.org/10.1016/j.jmmm.2005.02.043

[4] Mohri K, Honkura Y. Amorphous wire and CMOS IC based magneto-impedance sensors —Origin, topics, and future. Sensor Letters. 2007;**5**(1):267-270(4). DOI: https://doi.org/10.1166/sl.2007.082

[5] Kaniusas E, Mehnen L, Pfützner H. Magnetostrictive amorphous bilayers and trilayers for thermal sensors. Journal of Magnetism and Magnetic Materials. 2003;**254-255**:624-626. DOI: http://doi.org/10.1016/S0304-8853(02)00922-8

[6] Taylor GF. A method of drawing metallic filaments and a discussion of their properties and uses. Physical Review B. 1924;**23**:655-658. DOI: https://doi.org/10.1103/PhysRev.23.655

[7] Baranov SA. Evaluation of the distribution of residual stresses in the cord of amorphous microwire. Metal Science and Heat Treatment. 2001;**43**(3):167-168. DOI: 10.1023/A:1010569906136

[8] Vázquez M, Zhukov AP, Aragoneses P, Arcas J, Garcia-Beneytez JM, Marin P, Hernando A. Magneto-impedance in glass-coated CoMnSiB amorphous microwires. IEEE Transactions on Magnetics. 1998;**34**(3):724-728. DOI: 10.1109/20.668076

[9] Vázquez M. Magnetic bistability of amorphous wires and sensor applications. IEEE Transactions on Magnetics. 1994;**30**(2):907-912. DOI: 10.1109/20.312442

[10] Marín P, Vázquez M, Arcas J, Hernando A. Thermal dependence of magnetic properties in nanocrystalline FeSiBCuNb wires and microwires. Journal of Magnetism and Magnetic Materials. 1999;**203**(1-3):6-11. DOI: http://doi.org/10.1016/S0304-8853(99)00173-0

[11] Vázquez M, Marin P, Arcas J, Hernando A, Zhukov AP, González J. Influence of nanocrystalline structure on the magnetic properties of wires and microwires. Textures and Microstructures. 1999;**32**(1-4):245-267. DOI: dx.doi.org/10.1155/TSM.32.245

[12] Beach RS, Berkowitz AE. Giant magnetic field dependent impedance of amorphous FeCoSiB wire. Applied Physics Letters. 1994;**64**:3652. DOI: http://dx.doi.org/10.1063/1.111170

[13] Vazquez M, Chen DX. The magnetization reversal process in amorphous wires. IEEE Transactions on Magnetics. 1995;**31**(2):1229-1238. DOI: 10.1109/20.364813

[14] Kraus L, Infante G, Frait Z, Vázquez M. Ferromagnetic resonance in microwires and nanowires. Physical Review B. 2011;**83**:174438 (1)-174438 (11). DOI: https://doi.org/10.1103/PhysRevB.83.174438

[15] Marín P, Marcos M, Hernando A. High magnetomechanical coupling on magnetic microwire for sensors with biological applications. Applied Physics Letters. 2010;**96**:262512(1)-262512(3). DOI: http://dx.doi.org/10.1063/1.3459140

[16] Herrero-Gómez C, Marín P, Hernando A. Bias free magnetomechanical coupling on magnetic microwires for sensing applications. Applied Physics Letters. 2013;**103**:142414 (1)-142414(4). DOI: http://dx.doi.org/10.1063/1.4821777

[17] Marín P, Cortina D, Hernando A. High-frequency behavior of amorphous microwires and its applications. Journal of Magnetism and Magnetic Materials. 2005;**290-291**(2):1597-1600. DOI: https://doi.org/10.1016/j.jmmm.2004.11.255

[18] Makhnovskiy DP, Panina LV, Garc_ıa C, Zhukov A, González J. Experimental demonstration of tunable scattering spectra at microwave frequencies in composite media containing CoFeCrSiB glass-coated amorphous ferromagnetic wires and comparison with theory. Physical Review B. 2006;**74**:064205(1)-064205(11). DOI: 10.1103/PhysRevB.74.064205

[19] Luo Y, Peng HX, Qin FX, Ipatov M, Zhukova V, Zhukov A, Gonzalez J. Fe-based ferromagnetic microwires enabled meta-composites. Applied Physics Letters. 2013;**103**:251902. DOI: http://dx.doi.org/10.1063/1.4850196

[20] Marín P, Cortina D, Hernando A. Electromagnetic wave absorbing material based on magnetic microwires. IEEE Transactions on Magnetics. 2008;**44**(11):3934-3937. DOI: 10.1109/TMAG.2008.2002472

[21] Herrero-Gómez C, Aragón AM, Hernando-Rydings M, Marín P, Hernando A. Stress and field contactless sensor based on the scattering of electromagnetic waves. Applied Physics Letters. 2014;**105**:092405(1)-092405(4). DOI: http://dx.doi.org/10.1063/1.4894732

[22] Aragón AM, Hernando-Rydings M, Hernando A, Marín P. Liquid pressure wireless sensor based on magnetostrictive microwires for applications in cardiovascular localized diagnostic. AIP Advances. 2015;**5**:087132(1)-087132(7). DOI: 10.1063/1.4928605

[23] Hao Y, Foster R. Wireless body sensor networks for health-monitoring. Physical Meas.2008;**29**(11):R27-R56. DOI: 10.1088/0967-3334/29/11/R0

[24] Hernando Rydings M, Marín Palacios P, Aragón-Sánchez AM, Bravo Ruiz E, López-Domínguez V, Martínez López I, Fernández Pérez C, Bilbao González A, Javier Serrano Hernando F, Vega Manrique R, Hernando Grande A. Development of a telemetric system for postoperative follow-up of. Journal of the American Heart Association. 2016;**5**(e003608):1-12. DOI: 10.1161/JAHA.116.003608

[25] Taylor GF. A method for drawing metallic filaments and discussion of their properties and uses. Physical Review B. 1924;**23**:6555-6560. DOI: https://doi.org/10.1103/PhysRev.23.655

[26] Baranov AS, Larin VS, Torkunov AV, Zhukov AP, Vázquez M. Magnetic properties of glass insulated amorphous microwires. In: Vázquez M, Hernando A, editors. Nanocrystalline and Non-crystalline Materials. Singapore: World Scientific; 1995. pp. 567-571

[27] Gorriti AG, Marín P, Hernando A. Microwave power absorption by microwires under tensile stress. Sensor Letter. 2004;**7**(3):1-4. DOI: https://doi.org/10.1166/sl.2009.1058

[28] King RWP, Wu TT. The imperfectly conducting cylindrical transmitting antenna. IEEE Transactions on Antennas and Propagation. 1966;**14**(5):524-534. DOI: 10.1109/TAP.1966.1138733

[29] Makhnovskiy DP, Panina LV, Mapps DJ. Field-dependent surface impedance tensor in amorphous wires with two types of magnetic anisotropy: Helical and circumferential.

Physical Review B. 2002;**64**(14): 144424-144441. DOI: https://doi.org/10.1103/PhysRevB.63.144424

[30] Usov NA, Antonov AS, Lagarkov AN. Theory of giant magneto-impedance effect in amorphous wires with different types of magnetic anisotropy. Journal of Magnetism and Magnetic Materials. 1998;**185**:159-173. DOI: 10.1016/S0304-8853(97)01148-7

[31] Sandacci SI, Makhnovskiy DP, Panina LV. Valve-like behavior of the magnetoimpedance in the GHz range. Journal of Magnetism and Magnetic Materials. 2004;**272**:1855-1857. DOI: 10.1016/j.jmmm.2003.12.829

[32] Lofland SE, Bhagat SM, Dominguez M, García-Beneytez JM. Low-field microwave magnetoimpedance in amorphous microwires. Journal of Applied Physics. 1999;**85**(8): 4442-4444. DOI: http://dx.doi.org/10.1063/1.370368

[33] Makhnovskiy DP, Panina LV. Field dependent permittivity of composite materials containing ferromagnetic wires. Journal of Applied Physics. 2003;**93**:4120. DOI: http://dx.doi.org/10.1063/1.1557780

[34] Makhnovskiy DP, Panina LV, Garcia C, Zhukov AP, Gonzalez J. Experimental demonstration of tunable scattering spectra at microwave frequencies in composite media containing CoFeCrSiB glass-coated amorphous ferromagnetic wires and comparison with theory. Physical Review B. 2006;**74**:064205. DOI: https://doi.org/10.1103/PhysRevB.74.064205

[35] Hanson G. Fundamental transmitting properties of carbon nanotube antennas. IEEE Transactions on Antennas and Propagations. 2005;**53**(11):3426-3435. DOI: 10.1109/TAP.2005.858865

[36] Panina LV, Makhnovskiy DP, Morchenko AT. Tunable permeability of magnetic wires at microwaves. Journal of Magnetism and Magnetic Materials. 2015;**383**:120-125. DOI: 10.1016/j.jmmm.2014.11.051

[37] Hernando A, López-Domínguez V, Ricciardi E, Osiak K, Marín P. Tuned scattering of electromagnetic waves by a finite length ferromagnetic microwire. IEEE Transactions on Antennas and Propagations. 2016;**64**(3):1112-1115. DOI: 10.1109/TAP.2015.2513428

[38] Herrero-Gómez C, Aragón AM, Hernando-Rydings M, Marín P, Hernando A. Stress and field contactless sensor based on the scattering of electromagnetic waves by a single ferromagnetic microwire. Applied Physics Letters. 2014;**105**:092505(1)-092505(4). DOI: http://dx.doi.org/10.1063/1.4894732

[39] Hernando A, Vázquez M, Barandiarán JM. Metallic glasses and sensing applications. Journal of Physics E: Scientific Instruments. 1988;**21**(12):1129. DOI: https://doi.org/10.1088/0022-3735/21/12/002

[40] Jackson JD. Classical Electrodynamics. 3rd ed. New York: EEUU, Wiley; 1998